

Effect of the end-of-range loop layer depth on the evolution of {311} defects

R. Raman and M. E. Law^{a)}

SWAMP Center, Department of Electrical and Computer Engineering, University of Florida, Gainesville, Florida 32611-6130

V. Krishnamoorthy and K. S. Jones

SWAMP Center, Department of Materials Science and Engineering, University of Florida, Gainesville, Florida 32611-6130

(Received 17 July 1998; accepted for publication 30 November 1998)

The interactions between end-of-range dislocation loops and {311} defects as a function of their proximity were studied. The dislocation loops were introduced at 2600 Å by a dual $1 \times 10^{15} \text{ cm}^{-2}$, 30 keV and a $1 \times 10^{15} \text{ cm}^{-2}$, 120 keV Si^+ implantation into silicon followed by an anneal at 850 °C for 30 min. The depth of the loop layer from the surface was varied from 2600 to 1800 Å and 1000 Å by polishing off the Si surface using a chemical–mechanical polishing (CMP) technique. A post-CMP $1 \times 10^{14} \text{ cm}^{-2}$, 40 keV Si^+ implantation was used to create point defects at the projected range of 580 Å. The wafers were annealed at 700, 800, and 900 °C, and plan-view transmission electron microscopy study was performed. It was found that the number of interstitials in {311} defects decreased as the projected range damage was brought closer to the loop layer, while the number of rectangular elongated defects (REDs) increased. Experimental investigation showed that REDs are formed at the end of range. It is concluded that the interstitials introduced at the projected range are trapped at the end of range. The REDs are formed due to the interactions between the interstitials and the pre-existing dislocation loops. © 1999 American Institute of Physics. [S0003-6951(99)03705-5]

Transient enhanced diffusion of the implanted dopant during annealing occurs due to the implant damage, which evolves into a supersaturation of excess interstitials. The interstitials precipitate on {311} planes as a single monolayer of hexagonal Si giving rise to rod-like defects known as {311} defects running along $\langle 110 \rangle$ directions.^{1,2} Extended defects such as end-of-range (EOR) dislocation loops are formed at the amorphous/crystalline interface after a high dose amorphizing implant due to the existence of a supersaturation of interstitials in the region.³ These EOR dislocation loops affect the dopant distribution by capturing or releasing point defects during a subsequent thermal cycle. Because these processes are critical to the overall device performance requirements, a greater level of fundamental knowledge about the evolution of extended defects and their interactions with point defects is necessary. It has been shown that EOR dislocation loops are effective in capturing point defects generated from a low dose implant.^{4,5} The interaction kinetics between these dislocation loops and the introduced point defects has been shown to be diffusion limited and loops have been used to quantitatively measure the flux of the point defects.⁶

The goal of this experiment is to quantify the interactions between dislocation loops and interstitials introduced at the projected range as a function of their proximity. By maintaining an overlap at the shallowest loop depth of 1000 Å, it is hoped that the evolution of {311} defects in the presence of EOR loops can be better understood.

A 150 mm $\langle 100 \rangle$ Czochralski (CZ) grown *n*-type (8–30

Ω cm) Si wafer was implanted with 10^{15} cm^{-2} , 30 keV and a 10^{15} cm^{-2} , 120 keV Si^+ implant on an Eaton NV/GSD 200E implanter. The two overlapping implants were performed to produce a continuous surface amorphous layer. The tilt/twist angles for each implant were 5°/0°. Post-implantation annealing was performed in a furnace with flowing N_2 gas (99.999% purity) at 850 °C for 30 min. Cross-sectional transmission electron microscopy (XTEM) revealed that the band of EOR loops are approximately 300 Å wide and were formed at a depth of 2600 Å. The wafer was then diced into 1 cm×1 cm pieces on a Tempress® dicing saw. The chemical–mechanical polishing (CMP) procedure, developed by Herner, Gila, and Jones⁷ was used to polish the Si surface. The depths were verified using XTEM.

The loop samples were then implanted with 10^{14} cm^{-2} , 40 keV Si^+ to introduce the point defects at the projected range of 580 Å. Two types of control samples were used in this experiment. The {311} control sample was a dummy wafer which received the 10^{14} cm^{-2} , 40 keV Si^+ implant and had no dislocation loops. The loop control sample was an unpolished loop sample with pre-existing loops at 2600 Å. This sample did not receive the 10^{14} cm^{-2} , 40 keV Si^+ implant. The anneal times and temperatures were chosen based on prior knowledge of {311} dissolution times. The samples were furnace annealed at 700 °C (30 min, 5, and 10 h) and 800 °C (5, 10, and 20 min) and RTA (AG Associates Heat-pulse 2146) annealed at 900 °C (5, 30, and 60 s). All anneals were performed in flowing N_2 .

The PTEM image for the {311} control sample for the 700 °C, 30 min anneal is shown in Fig. 1(a). Figures 1(b), 1(c), and 1(d) show the PTEM images for the 2600, 1800,

^{a)}Electronic mail: law@tec.ufl.edu

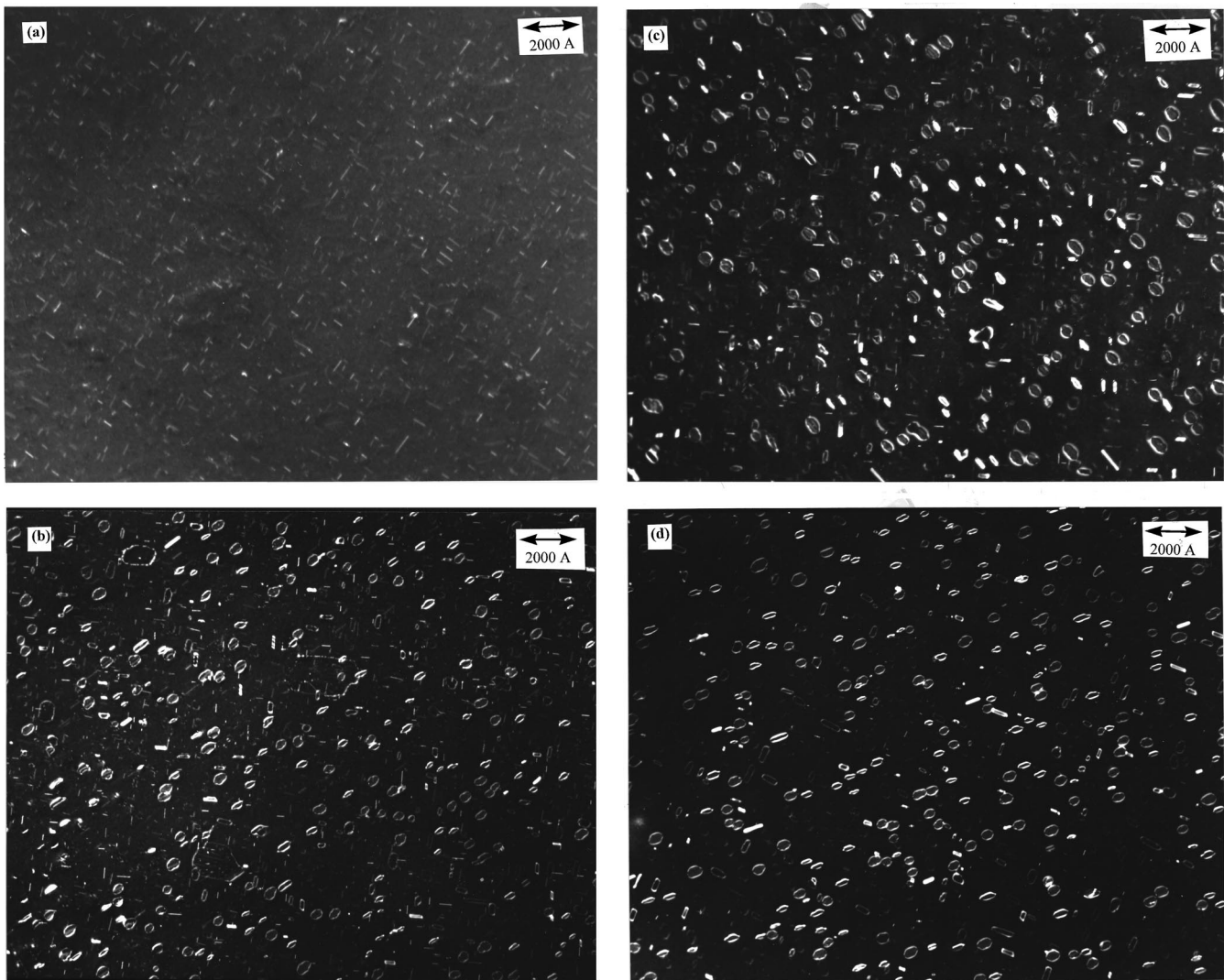


FIG. 1. PTEM images of (a) control sample, (b) loop depth at 2600 Å, (c) loop depth at 1800 Å, and (d) loop depth at 1000 Å.

and the 1000 Å loop samples, respectively, for the 700 °C, 30 min anneal. It can be seen from these four images that the density of {311} defects decreases from the {311} control sample down to the 1000 Å loop sample. Size distribution analysis revealed that the mean size of the {311} defects decreases as the projected range damage gets closer to the EOR dislocation loops. Figure 2 shows the plot of the number of interstitials trapped in {311} defects as a function of loop depth for the 700 °C, 30 min anneal. The number of interstitials trapped in {311} defects was extracted using the procedure developed by Bharatan.⁸ It was found that 4.5×10^{13} interstitials were trapped in {311} defects in the control sample. Interstitial counts from the loop samples showed that the number of interstitials trapped in {311} defects drops significantly with depth.

It was found that the number of rectangular elongated defects (REDs) had increased significantly in the shallow loop samples. Figure 3 shows a typical PTEM image of a set of REDs from the 1000 Å sample. From the area fraction occupied by the REDs, the number of interstitials trapped was extracted, assuming that the defects lie on the [111] plane just like circular loops. This result is shown in Fig. 2, presented together with the interstitial trend in {311} defects.

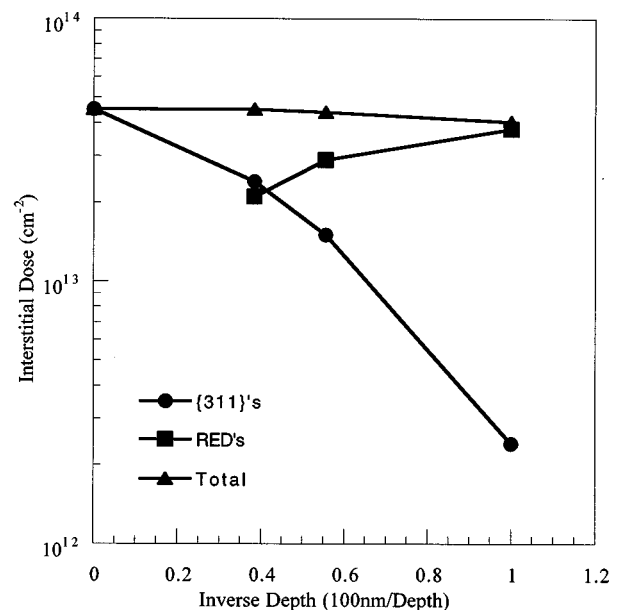


FIG. 2. Plot of the number of interstitials trapped in {311} defects and REDs as a function of loop depth.

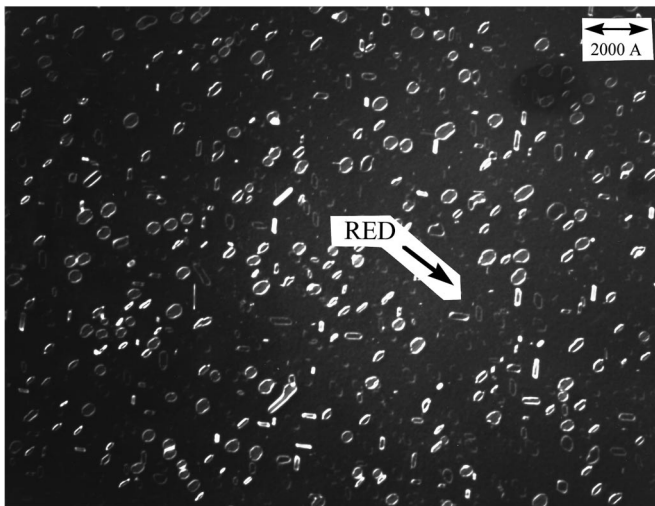


FIG. 3. PTM image showing the REDs.

Also shown in Fig. 2 is the total sum of interstitials in REDs and $\{311\}$ defects. It was found that the sum of the interstitials remains a constant within error. This sum is approximately equal to the total number interstitials in the $\{311\}$ control sample. This result suggests that the interstitials lost from $\{311\}$ defects were captured into the REDs. The results from the 800 and 900 °C anneals were also analyzed. It was found that the $\{311\}$ defects disappear very quickly at these temperatures and these samples showed the same trend as in the case of the 700 °C anneal.

Figure 4 shows the defect density of REDs, circular loops, and the total defect density (REDs+circular loops) as a function of loop depth, that the number of REDs have significantly increased in the 1000 Å loop sample in comparison to the density of circular loops which did not change significantly. The number of REDs has increased significantly beyond the expected sampling errors, which indicate that the REDs are new defects that are being nucleated.

Figures 2 and 4, when taken together are very surprising. The $\{311\}$ defects contain significantly fewer interstitials

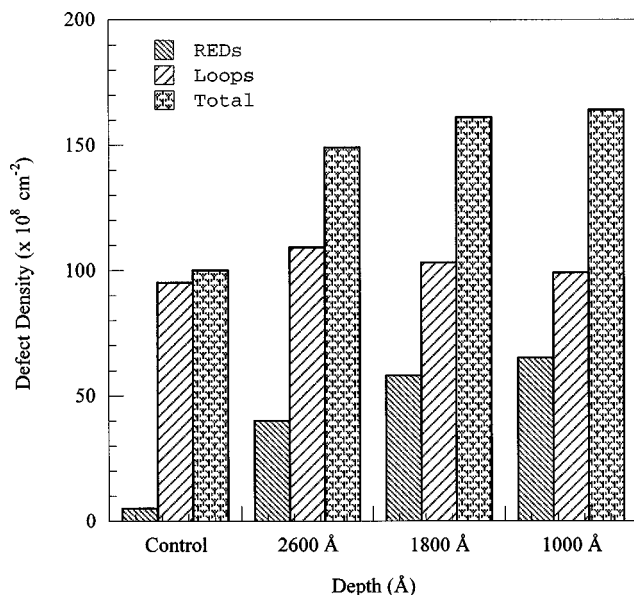


FIG. 4. Comparison of the defect density of REDs with the density of circular loops and the total defect density as a function of the loop depth.

when in close proximity to dislocation loops. The missing interstitials are trapped in the end-of-range on the REDs, as shown in Fig. 2. The natural assumption to make is that the interstitials are condensing on the existing dislocation loops. Figure 4, however, indicates that new defect structures are being formed. It appears, therefore, that the interstitials are not forming $\{311\}$'s and are not decorating existing loops. They prefer to form REDs as opposed to either of these mechanisms.

To determine if REDs are formed at the projected range or the end-of-range, two experiments were carried out. First, XTEM analysis was performed on the $\{311\}$ control sample and the three loop samples which showed no evidence of the existence of REDs in the projected range. Due to the high density of pre-existing EOR loops, it was hard to discern the REDs from the circular loops in the EOR region. To further clarify the location of these defects, CMP was performed on the 1000 Å sample to polish the Si surface down to the projected range. PTEM analysis was done on the CMP'ed sample and it was found that the density of REDs was not affected. This result suggests that these defects are formed at the end of range.

Using the CMP technique, the distance between the projected range damage and the EOR dislocation loops was varied without altering the loop density or distribution. This allowed us to study the interactions between interstitials introduced at the projected range and the EOR dislocation loops as a function of their proximity. It was found that when the projected range damage was farthest from the loop layer, a higher density of $\{311\}$ defects were formed. As the loops got closer to the projected range damage, the interstitials were increasingly trapped into REDs at the end of range. The sum of interstitials trapped in the $\{311\}$ defects and the REDs remains a constant for a given depth, suggesting that interstitials lost from $\{311\}$ defects prefer to nucleate REDs in the end-of-range loop layer as opposed to decorating existing dislocations or forming $\{311\}$ defects.

The authors would like to acknowledge NSF and SRC for funding this work.

¹K. S. Jones, J. Liu, L. Zhang, V. Krishnamoorthy, and R. T. DeHoff, Nucl. Instrum. Methods Phys. Res. B **106**, 227 (1995).

²D. J. Eaglesham, P. A. Stolk, H.-J. Gossmann, and J. M. Poate, Appl. Phys. Lett. **65**, 2305 (1994).

³K. S. Jones, S. Prussin, and E. R. Weber, Appl. Phys. A: Solids Surf. **45**, 1 (1988).

⁴J. K. Listerbarger, K. S. Jones, and J. A. Slinkman, J. Appl. Phys. **73**, 10 (1993).

⁵K. S. Jones, H. G. Robinson, J. Listerbarger, and J. Chen, Nucl. Instrum. Methods Phys. Res. B **96**, 196 (1995).

⁶H. Park, H. Robinson, K. S. Jones, and M. E. Law, Appl. Phys. Lett. **65**, 436 (1996).

⁷S. B. Herner, B. P. Gila, and K. S. Jones, J. Vac. Sci. Technol. B **14**, 6 (1996).

⁸S. Bharatan, J. Desroches, and K. S. Jones, in *Transmission Electron Microscopy Characterization of Lattice Damage* (Ion Beam, Austin, 1997).